Published in final edited form as:
Biochemistry. 2011 October 4; 50(39): 8323–8332. doi:10.1021/bi2009322.

Crystallographic Trapping of Heme Loss Intermediates During the Nitrite-Induced Degradation of Human Hemoglobin

Jun Yi[‡,*], **Leonard M. Thomas**[‡], **Faik N. Musayev**[§], **Martin K. Safo**[§], and **George B. Richter-Addo**[‡,*]

[‡]Department of Chemistry and Biochemistry, University of Oklahoma, Norman, Oklahoma 73019

[§]Department of Medicinal Chemistry, School of Pharmacy, Virginia Commonwealth University, Richmond, Virginia 23298

Abstract

Heme is an important cofactor in a large number of essential proteins and is often involved in small molecule binding and activation. Heme loss from proteins thus negatively affects the function of these proteins, but is also an important component of iron recycling. The characterization of intermediates that form during the loss of heme from proteins has been problematic due, in a large part, to the instability of such intermediates. We have characterized, by X-ray crystallography, three compounds that form during the nitrite-induced degradation of human $\alpha_2\beta_2$ hemoglobin (Hb). The first is an unprecedented complex that exhibits a large β heme displacement of 4.8 Å towards the protein exterior; the heme displacement is stabilized by the binding of the distal His residue to the heme Fe, which in turn allows for the unusual binding of an exogenous ligand at the proximal face of the heme. We have also structurally characterized complexes that display regiospecific nitration of the heme at the 2-vinyl position; we show that heme nitration is not a prerequisite for heme loss. Our results provide structural insight into a possible pathway for nitrite-induced heme loss from human Hb.

Keywords

iron; heme; binding; heme loss; nitrogen oxides; blood; hemoglobin

Heme is an important cofactor in a large number of essential proteins. Heme iron is directly involved in dioxygen binding and transport (1), and in gas sensing for signaling purposes (e.g., in NO signaling) (2). Xenobiotic detoxification and drug metabolism in the liver involve the heme in P450 enzymes (3). Heme cofactor dissociation from the proteins will thus be expected to negatively impact their function, although the dissociation is necessary for iron recycling. There are many reports describing the rates of heme dissociation from proteins (4-7). However, there is a paucity of molecular level information regarding the nature of the intermediates that form along the dissociation pathway.

[*]CORRESPONDING AUTHOR FOOTNOTE Address: Stephenson Life Sciences Research Center, 101 Stephenson Parkway, Norman, OK 73019. Telephone: (405) 325-2378. Fax: (405) 325-6111. yijun@ou.edu, grichteraddo@ou.edu. .

ACCESSION CODES: The coordinates have been deposited in the RCSB Protein Data Bank as entries 3ONZ ($Hb(ONO)_{d,p}$), 3OO4 (NαHb(ONO)) and 3OO5 (NHb(ONO)α).

Supporting Information Available. Supplemental Figures S1-S6. This material is available free of charge via the Internet at http://pubs.acs.org.

Author contributions J.Y. and G.B.R-A. designed research; J.Y., F.N.M., M.K.S., L.M.T. and G.B.R-A. performed research; J.Y., M.K.S., L.M.T. and G.B.R-A. analyzed data; and J.Y. and G.B.R-A. wrote the paper and coordinated coauthor feedback.

The authors declare no conflict of interest.

Human hemoglobin (Hb) is an important oxygen binding and transport protein that is active in the reduced ferrous form (1). The oxidized ferric form cannot bind oxygen nor transport it. Thus, factors that promote oxidation of Hb are of interest from a health perspective (8). Autoxidation of ferrous Hb converts it to the ferric form (9). Exogenous agents such as the ubiquitous nitrite anion (NO^-_2; pK_a 3.2 at 20 °C) (10) also oxidize Hb (11, 12). Indeed, nitrite poisoning can lead to methemoglobinemia (13) that is associated with an increase in ferric Hb (i.e., metHb) and its derivatives in the circulatory system. Interestingly, in vivo levels of nitrite have been estimated at ~300 nM in erythrocytes (14), but can be as high as 20 μM in vascular tissue (15).

The complexity of the Hb-nitrite interaction is derived from the ability of nitrite to oxidize ferrous Hb, bind to the heme center, covalently modify the heme, and degrade the protein via an as-yet undefined heme loss process. The first mention of a discrete Hb-nitrite complex with a direct Fe-nitrite bond was reported by Hartridge in 1920 (16), and early studies included those by Gibson and coworkers on the nitrite association kinetics on Hb and its isolated subunits (17). It wasn't until 2008, however, that the crystal structure of a discrete Hb-nitrite complex was reported; the structure revealed the existence of nitrito Fe-ONO moieties in both α and β subunits (Fig. S1) (18).

In the 1960s, Thompson and coworkers (19, 20) reported a discoloration of Hb to a green color upon treatment of Hb in solution with nitrite, and referred to the green pigment as "nitriheme". The biochemical characterization of the nitrihemoglobin (NHb) product was recently reported by Peterson and coworkers (21). In this latter report, nitration of the hemes in both the α and β subunits was suggested to occur in phosphate buffer based on mass spectral and spectroscopic data, consistent with what had been proposed previously by Timkovich (22) and Casella (23) for nitrimyoglobin. In his Ph.D. thesis, Bondoc (24) described his preliminary work on the formation of nitriHb in which only one of the (α or β) subunit hemes was nitrated, but there was insufficient information as to which subunit heme was nitrated. Peterson and coworkers noted that the formation of NHb was complete in phosphate buffer, but was incomplete in citrate buffer with accompanying precipitation of product (21). No three-dimensional structural characterization of nitriHb or any nitriheme protein has been reported to date. It is important to note that nitrite also degrades Hb into Heinz bodies (25, 26), and that Heinz body formation is normally associated with loss of heme from Hb. Curiously, however, no intermediates during the nitrite-induced heme loss process have been structurally characterized by X-ray crystallography. We note that lowering the pH of crystalline ferric horse Hb converts it into a hemichrome derivative in which its α subunit displays a bis-histidyl axial ligation with retention of the His/H_2O ligation in the β subunit (27). In addition, the guanidine hydrochloride-induced unfolding of ferric myoglobin generates a hemichrome derivative whose spectral properties are consistent with bis-histidyl axial ligation of the heme (7).

Given the complexity of the Hb-nitrite reaction (28-32), we embarked on a crystallographic study to identify possible intermediates that form during the nitrite-induced Hb degradation process. In this article, we describe the formation and X-ray crystallographic characterization of three compounds that display, in addition to nitrite binding to heme, structural modifications of the protein. The first is an unprecedented compound of Hb, obtained from solution during cocrystallization of Hb with nitrite, that displays a large β heme shift and exogenous ligand binding at the proximal binding site. In addition, and in order to unambiguously identify other products from this nitrite-induced degradation process (e.g., the green Hb products), we have structurally characterized two other products from crystal soaking experiments. These latter compounds display covalent modification of their heme cofactors in the α subunit alone, or in both α and β subunits.

MATERIALS AND METHODS

Human hemoglobin was isolated from blood (University of Oklahoma Health Sciences Center Emergency Room) and purified as oxyHb (33). Ferric aquometHb was obtained by treating oxyHb with excess ferricyanide (34).

The $Hb(ONO)_{d,p}$ derivative

OxyHb (in phosphate buffer, pH 7.0, 23 °C) was degassed under vacuum for 10 min in the presence of sodium dithionite to generate deoxyHb (33). Sodium nitrite was added to the protein solution, and the solution left to stand for 3 days to generate crystals of the $Hb(ONO)_{d,p}$ product.

Nitriheme derivatives

Crystals of ferric *R*-state aquometHb (18, 35) in 2.3 M phosphate buffer at 23 °C and pH 6.8 were soaked with excess sodium nitrite (0.16 M) for 16 h to give the α-nitriheme derivative NαHb(ONO) that displays nitriheme formation in the α subunit and nitrite binding to both α and β Fe atoms. Soaking crystals of ferric aquometHb crystals at 23 °C and pH 6.5 with the excess sodium nitrite for 8 days gave the α/β-nitriheme derivative NHb(ONO)α that displays nitriheme formation in both α and β subunits but nitrite binding to only the α subunit.

Structure determination

Crystals of all three derivatives above were harvested using cryoloops, soaked in mother liquor containing 16% glycerol, and flash-frozen in liquid nitrogen prior to data collection. Diffraction data were collected at 100 K on Rigaku RU3HR (University of Oklahoma) or RU-200 (Virginia Commonwealth University) rotating anode X-ray generators (CuKα radiation). Diffraction data were processed with either *d*TREK* (36) or *iMosflm* (37) Phase information was obtained by molecular replacement using the 2.1 Å resolution structure of human HbCO (PDB accession code 1LJW; with solvent and CO removed) as the search model. Refinement was carried out using *REFMAC* (38) and *PHENIX* (39). Simulated annealing, as implemented in *PHENIX*, was utilized to reduce model bias during the initial stages of refinement. The Fe-nitrite bond distance and angle parameters were unrestrained throughout the refinement; however, internal restraints of 1.25(2) Å (for *d*(N-O)) and 119(3)° (for ∠ONO) were applied to the nitrite group. Bulk-solvent modeling and isotropic scaling of the observed and calculated structural amplitudes were used during the restrained refinements. *COOT* (40) was used for visualization and model building/correction between refinement cycles. Water molecules were added to the structures at the final stages of the refinements using the *Update Waters* command in *PHENIX*. Data collection and structure refinement statistics are provided in Table 1.

For the $Hb(ONO)_{d,p}$ structural determination, the initial electron density map revealed the presence of an Fe ligand in the sixth position for the α subunit. A nitrite anion was modeled into this electron density. The distal pocket of the β subunit showed what appeared to be a heme group that had shifted laterally towards the exterior in the direction of the distal His63 sidechain. In addition, there was undefined electron density in the proximal helix region. A heme group was modeled into this shifted position (initially at ~4.5 Å away from its original position). A subsequent electron density map revealed residual electron density near the original Fe position of this β subunit. To evaluate the likelihood that the density was due to a subpopulation of heme in its original position, the *SFALL* and *FFT* programs were used to calculate the Fe anomalous signals for this structure. In the anomalous map, there were two positive electron density peaks in the heme moiety with an intensity ratio of ~3:7, thus confirming that these signals were both from Fe in two positions (Fe_1 for the "original" heme site, and Fe_2 for the shifted heme that was 4.8 Å shifted from its original position).

Due to a lack of defined electron density on the unshifted heme group, we only modeled the major (shifted) heme contribution at 62% occupancy based on the Fe anomalous signal ratio. The Fe_1 atom was modeled into the anomalous electron density at 28% occupancy; for an overall β heme occupancy of 90%. We were unable to properly model residues 88-91 and 93-97 in the proximal F helix in the β subunit due to undefined electron density in this region. However, the His92 residue was fairly well defined in the electron density map; this is the normal proximal ligand to Fe in the unshifted heme. V-shaped electron density was observed at the proximal side of the shifted heme, in contact with the Fe_2 atom. A nitrite ligand was modeled into this density at equivalent occupancy as the shifted heme (at 62%).

For the NαHb(ONO) structural determination, the initial electron density map revealed the presence of Fe ligands in the sixth positions for both the α and β subunits. Nitrite anions were modeled into this electron density. In addition, positive electron density (slightly V-shaped) was present at the 2-vinyl position of the heme in the α subunit. The *SMILE* program (as implemented in *COOT*) was used to generate the O=N-O molecule pdb file and the library file. This nitro group was modeled into the V-shaped density at the 2-vinyl position of the heme in the α subunit. The resulting modified heme cofactor (α subunit alone) was then used in subsequent refinements using *PHENIX*. This nitro group was modeled at 80%; when modeled at 100%, some negative electron density at this (nitro) position was observed in the resulting electron density map. The modified heme cofactor group has been assigned the NTE three-letter code in the PDB file.

For the NHb(ONO)α structural determination, the initial electron density map revealed the presence of an Fe ligand in the sixth position for the α subunit. A nitrite anion was modeled into this electron density. In addition, clear positive electron density was present at the 2-vinyl position of this α heme similar to that in the NαHb(ONO) structure described above; the modified heme cofactor was similarly modeled as a nitriheme. The distal pocket of the β subunit showed, from the electron density map, a relatively undefined heme electron density that appeared to result from the contributions of more than one heme in difference lateral locations. In addition, two positive electron density regions were present around the β heme site. Assuming a single heme occupancy, one of the positive electron density regions was at the 2-vinyl position of the heme, and the other near the γ-meso position. To evaluate the possibility that the density was due to a subpopulation of hemes that had moved laterally towards the exterior, the *SFALL* and *FFT* programs were used to calculate the Fe anomalous signals for this structure. In the anomalous map, there were two positive electron density peaks in the β heme moiety with an intensity ratio of 6:4, thus confirming that these signals were both from Fe in two positions (Fe_1 for the “original” heme site, and Fe_2 for the shifted heme). Due to a lack of defined electron density on the shifted heme group, we only modeled the major heme (Fe_1) contribution at 60% occupancy based on the Fe anomalous signal ratio. The Fe_2 atom was modeled into the anomalous electron density with a distance of 4.6 Å away from the Fe_1 site in this β subunit. As observed in the α subunit, additional electron density at the 2-vinyl position of the heme (Fe_1) was present; a nitro group was modeled into this electron density, also at 60% occupancy, to generate a nitriheme cofactor. No defined electron density was observed for a sixth Fe-ligand of the heme in the β subunit.

RESULTS

Incubation of Hb with nitrite results in the generation of several species. One of these products (termed $Hb(ONO)_{d,p}$) was obtained from solution as red crystals; during this cocrystallization experiment, several other species were generated as a green heterogeneous mixture that was difficult to crystallize. We adapted our isolation strategy and utilized crystal soaking (with nitrite) experiments to obtain and structurally characterize two other

compounds (termed NαHb(ONO) and NHb(ONO)α) from this reaction of Hb with nitrite. We now describe the isolation and structural characterization of the three compounds.

Proximal Fe-ligand interaction associated with a large β heme movement in Hb: The $Hb(ONO)_{d,p}$ compound

Cocrystallization of deoxyHb with excess nitrite under aerobic conditions for 3 days gave a product whose crystal structure revealed unprecedented features in Hb structural biology. The initial difference electron density map suggested the presence of a nitrite ligand bound to Fe of the α heme, similar to that determined previously for ferric *R*-state Hb(ONO) (18). The nitrite ligand in the α subunit was modeled in the *trans* O-binding mode with an Fe–O–N–O torsion angle of 168°. The $2F_o$-F_c electron density map fitted with the final refined model of this new product is shown at the top of Fig. 1. The related F_o-F_c omit electron density map is shown at the bottom of Fig. 1. The latter map was generated by removing, from the final model, the nitrite ligands (from both α and β subunits), and the heme group and one water molecule (from the β subunit), followed by subsequent refinement.

Major differences in the β subunit of this product from other Hb structures described in the literature are evident. First, two Fe positions (labeled Fe_1 and Fe_2) were calculated from the Fe anomalous signals from the diffraction data (see Fig. S2). The ratio of the Fe_1 (unshifted) and Fe_2 (shifted) atoms was 3:7. This was consistent with the fact that the electron density we observed in the β heme environment could not be readily explained by presence of a single heme. Although we modeled two Fe atom positions, we were only able to effectively model the heme macrocycle associated with the major (shifted) Fe_2 position as shown on the right of Fig. 1. Second, the distal His63 residue makes contact with the Fe_2 atom with a Fe_2–N distance of 2.3 Å. Third, the proximal His92 residue essentially remains in its general position but its pyrrole plane is rotated by 40°; the closest non-bonding N(His92)-to-C(shifted heme pyrrole) distance is 2.8 Å. Fourth, significant unwinding of the proximal F helix in this β subunit is deduced by the lack of clear electron density for the residues 88–91 and 93–97. Lastly, and most unexpectedly, electron density at the new proximal position of the shifted heme was consistent with the presence of nitrite at this position. The Fe_2–O(nitrite) distance of 3.0 Å suggests an electrostatic interaction between these moieties. We name this product $Hb(ONO)_{d,p}$ to reflect both distal (α subunit) and proximal (β subunit) Fe-nitrite interactions.

Regiospecific nitration of α heme in Hb: The NαHb(ONO) compound

We then sought to establish the identities of other nitrite-modified derivatives. We were not successful in obtaining suitable crystals of these pre-formed compounds from solution, as it appears that they form simultaneously as a heterogenous green mixture. We thus adapted our strategy to employ crystal soaking experiments to increase our chances of success at obtaining these species. Exposure of crystals of ferric *R*-state aquometHb at pH 6.8 to nitrite for 16 h resulted in the formation of a new red-green product. The F_o-F_c omit electron density map (generated by removing nitrite ligands from the final model) and final model of the structure of the product is shown at the top of Fig. 2.

The bulk features of the distal pockets in this product were similar to that determined previously for ferric *R*-state Hb(ONO) (18). The nitrite ligands in the distal pockets were modeled in the O-binding mode with Fe–O–N–O torsion angles of 166° (α subunit; *trans* conformation) and −93° (β subunit). In addition, new electron density at the 2-vinyl position of the heme in the α subunit was observed. No such new electron density at this position was observed in the β subunit. A nitro group was modeled into this new electron density in the α subunit (at 80% occupancy) to generate a nitriheme moiety. Fig. 3 (right) shows the top view of the α nitriheme and the electron densities associated with the nitrite ligand and the

nitriheme functional group at the 2-vinyl position; the numbering scheme is based on the IUPAC recommendations using the Fisher system (left of Fig. 3). Importantly, the covalent modification of the vinyl heme substituent by nitrite was regiospecific, and the 2-nitrovinyl moiety was found to be essentially coplanar with the adjacent pyrrole ring suggesting extended conjugation with this group.

Regiospecific nitration of both α and β hemes in Hb: The NHb(ONO)α compound

When crystals of *R*-state ferric aquometHb are soaked with nitrite at pH 6.5 for an extended period (1 week), a different product is obtained. The F_o-F_c omit electron density map (generated by removing the nitro group at the 2-vinyl position in the α subunit and nitrite ligands from the final model) and the final model of this structure of the new dark green crystalline product is shown at the bottom of Fig. 2.

The bulk features of the distal pocket of the α subunit of this product are similar to that described above for the α subunit of the NαHb(ONO) derivative (top left of Fig. 2), namely the nitrite ligand O-binding to Fe in the *trans* conformation and the α nitriheme modification. The heme environment of the β subunit is, however, markedly different. Fe was observed in two positions in the β distal pocket, in a 6:4 (Fe_1:Fe_2) ratio, calculated from the Fe anomalous signals from the diffraction data (see Fig. S3). Somewhat similar to the $Hb(ONO)_{d,p}$ structure, and although we modeled two Fe atom positions, we were only able to effectively model the heme macrocycle associated with the Fe_1 position (major position, unshifted; 60% occupancy) as shown on the bottom right of Fig. 2. For this major heme position, electron density consistent with the formation of a 2-nitrovinyl covalent modification was also evident, and this was modeled as such. No electron density for an Fe-bound nitrite ligand was evident in the β subunit.

DISCUSSION

Nitrite-induced degradation in Hb

It is surprising that despite the many studies reported regarding nitrite-induced degradation of Hb, there was no structural information on the nature of intermediates that could form during this process. We thus focused on obtaining such structural information by employing single-crystal X-ray crystallography.

The $Hb(ONO)_{d,p}$ product obtained from cocrystallizing Hb with nitrite shows two striking features: (i) a large ~4.8 Å lateral shift of the β heme towards the protein exterior, and (ii) proximal ligand binding to tetrameric Hb. The superposition of the β heme environment of $Hb(ONO)_{d,p}$ with that of the previously reported Hb(ONO) compound (PDB accession code 3D7O) (18) is shown in Fig. 4. The new Fe_2 atom position is shifted 4.8 Å from its original location, and the heme shift is accompanied by a 15° anticlockwise (when viewed from the distal side) in-plane rotation. This is the largest reported heme slippage for human tetrameric Hb. For comparison, a heme Fe shift of ~3.1 Å towards the protein exterior has been observed in the α-Hb-AHSP complex (AHSP is the α-Hb stabilizing protein) (41). A heme shift of 2.0 Å was observed when CO ligates murine neuroglobin (42), and a ~1.2 Å heme shift towards the protein exterior was observed during the acid-induced hemichrome (bis-histidyl) formation in horse Hb (27).

Remarkably, the exogenous ligand (nitrite) in $Hb(ONO)_{d,p}$ interacts with the β-heme via the proximal side of the heme (Fig. 1, right). We could not find precedent for the proximal interactions of exogenous ligands with human tetrameric $\alpha_2\beta_2$ Hb. All reported ligand binding studies on human tetrameric Hb refer to the binding of the ligands at the distal side of the heme. A somewhat related example we could locate was the observation of proximal dioxygen binding to the isolated α-Hb subunits in the α-Hb-AHSP complex (41). Fago and

coworkers reported NO binding to a human Hb mutant (namely the αH87G mutant lacking a proximal His ligand) to give the five-coordinate nitrosyl heme at the α subunit (43). However, we note that all five-coordinate α-FeNO derivatives of human Hb that have been characterized by X-ray crystallography display distal binding of NO to the heme center (44).

Clues as to why the β subunits have a greater propensity than the α subunits to be reactive with nitrite towards heme slippage may be found in earlier studies on Hb heme exchange and reconstitution studies. Gibson and coworkers reported that nitrite reacted faster with isolated Hb β chains about six times faster than with the isolated α chains (17). Hargrove and coworkers (4) have shown that heme dissociation from Hb β subunits is faster than from α subunits, consistent with earlier findings by Bunn and Jandl (6, 45). Further, Yonetani and coworkers (46) revealed a more facile dissociation of protoporphyrin (PP) from the β chains of the hybrid Hbs $\alpha(Fe)_2\beta(PP)_2$ and $\alpha(PP)_2\beta(Fe)_2$, and suggested a higher affinity of the α globin for PP than the β globin. Others have reported the formation of bis-histidyl hemichromes from the reaction of nitrite with isolated Hb subunits (47). However, we did not encounter hemichrome formation in our work with tetrameric Hb.

It is interesting to note that heme slippage occurs within crystals of NHb(ONO)α with the major β-nitriheme position in its original unshifted position. We note, however, that we have not yet been able to crystallize preformed NHb from solution. In cocrystallized $Hb(ONO)_{d,p}$, no nitriheme was present in the structure, and the major component of the β-heme was in the shifted position. It is apparent from these results that the nitrite-induced heme slippage observed is thus not dependent on prior formation of the nitriheme. The consequences of the β-heme slippage on the overall structures of both NHb(ONO)α and $Hb(ONO)_{d,p}$ are illustrated in the overlay shown in Fig. S4. In general, large atomic displacements of the mainchain Cα atoms in the E–F helix region of the β subunits (relative to the Cα atoms of the reference compound ferric aquometHb) are observed for both NHb(ONO)α and $Hb(ONO)_{d,p}$, and this reveals an inherent flexibility of the β-subunit in its reactions with nitrite. In fact, larger Cα displacements are observed in the E–F regions of the β-subunits even in the “discrete” Hb(ONO) complex reported earlier(18) that did not display heme slippage; this suggests a greater likelihood of heme movement in this subunit during follow-up reactions with the nitrite reagent.

Origin of regiospecificity of nitriheme formation

In principle, nitration of the hemes in Hb could occur either at the 2-vinyl or 4-vinyl positions, or at the meso carbon (methine) positions. What factors thus contribute to the regiospecificity in the 2-vinyl nitration observed for human Hb? To answer this question, we examined the distal pocket environments of the precursor *R*-state aquometHb as determined by crystallography (35). Fig. 5 shows the closet contacts between the terminal C-atoms of the two heme vinyl groups with the Cα protein chain backbone (top two panels) and the sidechains (lower two panels) in the more readily nitrated α subunits. The Cα atoms of the protein backbone in the vicinity of the 4-vinyl position (Fig. 5A) are, in general, closer to the terminal C-atom of the 4-vinyl group than are the Cα atoms from the 2-vinyl group in the β subunit (Fig. 5B). Further, the number of nearest contacts (<5 Å) between the 4-vinyl group and the distal pocket sidechains (Fig. 5C) are more than those of the 2-vinyl group (Fig. 5D). Both these observations in the crystal structure of the *R*-state aquometHb precursor point to the probable role of protein sterics in directing the nitration to the 2-vinyl position, and subsequently explain why the 2-vinyl nitration was favored over the 4-vinyl nitration. A similar situation exists for the description of the β subunit sterics (Fig. S5). Consistent with the hypothesis that sterics drive the stereospecificity is that nitration at the 2-vinyl position does not significantly perturb the positions of the neighboring residues (Fig. S6).

We note that nitriheme formation in Mb was also reported to be regiospecific at the 2-vinyl position (as observed for NαHb(ONO); Fig. 3) primarily on the basis of NMR spectroscopy (22); a similar proposal was made for Hb (21). On the other hand, nitration of the non-natural octaethylporphyrin and a synthetic *meso*-porphyrin dimethyl ester with acidified nitrite occurred primarily at the porphyrin *meso* positions (i.e., at the methine-*CH* positions) (48). Acidified nitrite reacted with heptaethylvinylporphyrin at the vinyl position to give a nitrovinyl product (49); heme vinyl nitration with tetranitromethane has also been reported (50). Interestingly, the related reaction of acidified nitrite with protoporphyrin IX dimethyl ester (PPDME) gave two isolable nitrated-at-vinyl products that were green in color, namely the 4-nitrovinyl and 2-nitrovinyl products (49). The small-molecule crystal structure of the 4-nitrovinyl product was determined to confirm its formulation. The related reaction of PPIX with acidified nitrite gave a mixture of green nitrated-at-vinyl and red nitrated-at-methine products (22). Hollenberg and coworkers reported (51), on the basis of UV-vis and HPLC-MS results, that a nitration of the heme in cytochrome P450 2B6 occurs when the enzyme is reacted with peroxynitrite; however, the site of nitration was not explicitly determined. It is thus reasonable to predict, based on our X-ray crystallographic results for Hb, that similar heme nitration regiospecificities may be induced by the immediate protein environments on the vinyl groups.

Several pathways may be envisaged for nitriheme formation from acidified nitrite. Importantly, the rate of nitration of the heme in Hb has been found to be dependent on nitrite, protons, and oxygen concentrations (21); the authors proposed a mechanism that involves an N_2O_5 intermediate that forms from attack of nitrite on a heme-NO_2 species. Acidified nitrite is a source of nitrous acid and the nitrosonium cation (NO^+) (52). Alternatively, therefore, electrophilic substitution at a vinyl (olefinic) group by the nitrosonium ion could generate an unstable nitrosovinyl intermediate (i.e., C=C(N=O)H) (53) which could be subsequently oxidized by air or nitrite to give the nitrated product. There is chemical precedent for the apparent direct nitration of olefins by nitrites. Kunai and coworkers (54) reported that sodium nitrite reacted with cyclohexene under weakly acidic conditions over several hours to give low yields of nitrocyclohexene; the reaction was enhanced by electrolysis. Further, Yandovskii and coworkers (55) showed that alkyl nitrites reacted with terminal olefins to give moderate yields of the nitrated products (with the nitro group at the terminal positions). We are unsure if the mechanism previously determined for NHb formation in solution (21) is operative in our crystal reactions.

Implications for the mechanism of heme loss

Nitrite oxidizes ferrous heme and also induces the formation of Heinz bodies. Thus, the observation of the β-heme shifting in our Hb-nitrite reactions begs the question “does heme shifting and loss from the β subunit precede nitrite-induced Heinz body formation?”. We were surprised to find that there was not much information in the literature regarding proposed molecular-level pathways for the nitrite-induced heme loss from Hb or similar globins.

Our results thus provide insight into a possible pathway for the nitrite-induced heme loss from Hb. In principle, however, there are many intermediates and transition states that can be envisaged to form during this heme loss process. Our crystallographic results, for both $Hb(ONO)_{d,p}$ and NHb(ONO)α, suggest that a likely stable intermediate is that in which the displaced heme is “trapped” by the distal His at a distance of 4.6–4.8 Å from its original position, and that nitriheme formation is not a prerequisite for this heme shifting. This heme shifting allows the distal His to now contact the new iron (Fe_2) position by swinging out towards the solvent edge, and allows a new proximal Fe-ligand bond to form (where the ligand is an exogenous ligand, solvent, or protein ligand); in the case of $Hb(ONO)_{d,p}$, this intermediate is trapped for crystallographic characterization by an exogenous proximal

nitrite ligand. Indeed, the breakage of the initial proximal Fe-His bond in $Hb(ONO)_{d,p}$ would imply that the protein's function has already been compromised at this stage of the degradation process; further heme displacement would thus lead to eventual heme removal and protein destabilization. Support for our hypothesis of the role of β-heme shifting and eventual loss as obligatory steps in β-subunit degradation comes from the following two observations. Various mutant Hbs (e.g., Koln, Hammersmith, San Francisco, and Zurich) that contain mutations in the β subunits near the heme that enhance heme dissociation from the β subunits of these mutants also degrade to form Heinz bodies (56, 57), and the $\alpha_2(h)\beta_2(o)$ hybrid that contains heme in the α subunits but not in the β subunits precipitates is known to precipitate into Heinz bodies (58).

CONCLUSIONS

Our results demonstrate, at a molecular level, the inherent complexity of the Hb-nitrite reaction. We have crystallographically trapped intermediates along the heme loss pathway for two Hb derivatives, namely $Hb(ONO)_{d,p}$ and NHb(ONO)α; these results provide a molecular level insight into a possible pathway for nitrite-induced heme loss from human tetrameric Hb. In addition to direct binding of the nitrite anion to heme Fe, nitrite can also induce a covalent and regiospecific modification of the 2-vinyl position of the heme to generate a green 2-nitrovinyl heme (i.e., nitriheme) cofactor. Further reaction of this nitriheme derivative with nitrite can induce heme shifting in the β-subunit, although nitriheme formation is not a prerequisite for heme shifting. Importantly, several blood borne diseases such as malaria are associated with heme loss events from Hb during parasite invasion. Thus, we are investigating whether similar intermediates as those isolated in this study can be obtained in those studies.

Supplementary Material

Refer to Web version on PubMed Central for supplementary material.

Acknowledgments

We are grateful to Professor Takashi Yonetani for helpful discussions and insight into hemoglobin structure-function.

† Supported by the Oklahoma Center for the Advancement of Science and Technology (HR9-081 to GBR-A) and the National Institutes of Health (GM 064476 to GBR-A).

LIST OF ABBREVIATIONS

AHSP	α-hemoglobin stabilizing protein
aquometHb	oxidized (ferric) form of hemoglobin containing an axial water ligand
Hb	hemoglobin
metHb	oxidized (ferric) form of hemoglobin
Mb	myoglobin
NHb	nitrihemoglobin
nitriheme	protoporphyrin IX derivative with a 2-nitrovinyl substituent
PDB	Protein Data Bank
PPDME	protoporphyrin IX dimethyl ester

PPIX protoporphyrin IX

REFERENCES

1. Yonetani T, Laberge M. Protein Dynamics Explain the Allosteric Behaviors of Hemoglobin. Biochim. Biophys. Acta. 2008; 1784:1146–1158. [PubMed: 18519045]
2. Boon EM, Marletta MA. Ligand Specificity of H-NOX Domains: From sGC to Bacterial NO Sensors. J. Inorg. Biochem. 2005; 99:892–902. [PubMed: 15811506]
3. Guengerich, FP., editor. Human Cytochrome P450 Enzymes. 3rd Ed. Kluwer Academic/Plenum; New York: 2005.
4. Hargrove MS, Singleton EW, Quillin ML, Ortiz LA, Phillips GN, Olson JS, Mathews AJ. His(64) (E7)→Tyr Apomyoglobin as a Reagent for Measuring Rates of Hemin Dissociation. J. Biol. Chem. 1994; 269:4207–4214. [PubMed: 8307983]
5. Hargrove MS, Wilkinson AJ, Olson JS. Structural Factors Governing Hemin Dissociation from Metmyoglobin. Biochemistry. 1996; 35:11300–11309. [PubMed: 8784184]
6. Bunn HF, Jandl JH. Exchange of Heme Among Hemoglobins and Between Hemoglobin and Albumin. J. Biol. Chem. 1968; 243:465–475. [PubMed: 4966113]
7. Culbertson DS, Olson JS. Role of Heme in the Unfolding and Assembly of Myoglobin. Biochemistry. 2010; 49:6052–6063. [PubMed: 20540498]
8. Percy MJ, McFerran NV, Lappin TRJ. Disorders of Oxidized Haemoglobin. Blood Rev. 2005; 19:61–68. [PubMed: 15603910]
9. Shikama K. The Molecular Mechanism of Autoxidation for Myoglobin and Hemoglobin: A Venerable Puzzle. Chem. Rev. 1998; 98:1357–1373. [PubMed: 11848936]
10. Braida W, Ong SK. Decomposition of Nitrite Under Various pH and Aeration Conditions. Water, Air, and Soil Pollution. 2000; 118:13–26.
11. Doyle MP, Pickering RA, DeWeert TM, Hoekstra JW, Pater D. Kinetics and Mechanism of the Oxidation of Human Deoxyhemoglobin by Nitrites. J. Biol. Chem. 1981; 256:12393–12398. [PubMed: 7298665]
12. Keszler A, Piknova B, Schechter AN, Hogg N. The Reaction Between Nitrite and Oxyhemoglobin. J. Biol. Chem. 2008; 283:9615–9622. [PubMed: 18203719]
13. Titov VY, Petrenko YM. Proposed Mechanism of Nitrite-Induced Methemoglobinemia. Biochemistry (Moscow). 2005; 70:473–483. [PubMed: 15892615]
14. Grubina R, Huang A, Shiva S, Joshi MS, Azarov I, Basu S, Ringwood LA, Jiang A, Hogg N, Kim-Shapiro DB, Gladwin MT. Concerted Nitric Oxide Formation and Release from the Simultaneous Reactions of Nitrite with Deoxy- and Oxyhemoglobin. J. Biol. Chem. 2007; 282:12916–12927. [PubMed: 17322300]
15. Vanin AF, Bevers LM, Slama-Schwok A, van Faassen EE. Nitric Oxide Synthase Reduces Nitrite to NO under Anoxia. Cell. Mol. Life Sci. 2007; 64:96–103. [PubMed: 17160351]
16. Hartridge H. Nitrite Methaemoglobin and Related Pigments. J. Physiol. 1920; 54:253–259. [PubMed: 16993466]
17. Gibson QH, Parkhurst LJ, Gerachi G. The Reaction of Methemoglobin with Some Ligands. J. Biol. Chem. 1969; 244:4668–4676. [PubMed: 5808510]
18. Yi J, Safo MK, Richter-Addo GB. The Nitrite Anion Binds to Human Hemoglobin via the Uncommon *O*-Nitrito Mode. Biochemistry. 2008; 47:8247–8249. [PubMed: 18630930]
19. Fox JB, Thomson JS. Formation of Bovine Nitrosylmyoglobin. I. pH 4.5-6.5. Biochemistry. 1963; 2:465–470. [PubMed: 14069530]
20. Fox JB, Thomson JS. The Formation of Green Heme Pigments from Metmyoglobin and Methemoglobin by the Action of Nitrite. Biochemistry. 1964; 3:1323–1328. [PubMed: 14229676]
21. Otsuka M, Marks SA, Winnica DA, Amoscato AA, Pearce LL, Peterson J. Covelent Modifications of Hemoglobin by Nitrite Anions: Formation Kinetics and Properties of Nitrihemoglobin. Chem. Res. Toxicol. 2010; 23:1786–1795. [PubMed: 20961082]

22. Bondoc LL, Timkovich R. Structural Characterization of Nitrimyoglobin. J. Biol. Chem. 1989; 264:6134–6145. [PubMed: 2703482]
23. Nicolis S, Pennati A, Perani E, Monzani E, Sanangelantoni AM, Casella L. Easy Oxidation and Nitration of Human Myoglobin by Nitrite and Hydrogen Peroxide. Chem. Eur. J. 2006; 12:749–757.
24. Bondoc, LL. Ph.D. Thesis. The University of Alabama; Tuscaloosa, Alabama: 1989. The Structures of Unusual Porphyrins and Hemes: Sulfmyoglobin and Nitrimyoglobin; p. 212-217.
25. Rifkind JM, Abugo O, Levy A, Heim J. Detection, Formation, and Relevance of Hemichromes and Hemochromes. Methods Enzymol. 1994; 231:449–480. [PubMed: 8041268]
26. Blumberg WE, Peisach J. Low-Spin Compounds of Heme Proteins. Adv. Chem. Ser. 1971; 100:271–291.
27. Robinson VL, Smith BB, Arnone A. A pH-Dependent Aquomet-to-Hemichrome Transition in Crystalline Horse Methemoglobin. Biochemistry. 2003; 42:10113–10125. [PubMed: 12939139]
28. Gladwin MT, Grubina R, Doyle MP. The New Chemical Biology of Nitrite Reactions with Hemoglobin: *R*-State Catalysis, Oxidative Denitrosylation, and Nitrite Reductase/Anhydrase. Acc. Chem. Res. 2008; 42:157–167. [PubMed: 18783254]
29. Roche CJ, Dantsker D, Samuni U, Friedman JM. Nitrite Reductase Activity of Sol-Gel-encapsulated Deoxyhemoglobin: Influence of Quatenary and Tertiary Structure. J. Biol. Chem. 2006; 281:36874–36882. [PubMed: 16984908]
30. Nagababu E, Ramasamy S, Rifkind JM. Intermediates Detected by Visible Spectroscopy During the Reaction of Nitrite with Deoxyhemoglobin: The Effect of Nitrite Concentration and Diphosphoglycerate. Biochemistry. 2007; 46:11650–11659. [PubMed: 17880185]
31. Kohn MC, Melnick RL, Ye F, Portier CJ. Pharmacokinetics of Sodium Nitrite-Induced Methemoglobinemia in the Rat. Drug Metab. Disposit. 2002; 30:676–683.
32. Hopmann KH, Cardey B, Gladwin MT, Kim-Shapiro DB, Ghosh A. Hemoglobin as a Nitrite Anhydrase: Modeling Methemoglobin-Mediated N_2O_3 Formation. Chem. Eur. J. 2011; 17:6348–6358.
33. Safo MK, Abraham DJ. X-ray Crystallography of Hemoglobins. Methods Mol. Med. 2003; 82:1–19. [PubMed: 12669634]
34. Antonini, E.; Brunori, M. Hemoglobin and Myoglobin In Their Reactions With Ligands. North-Holland; Amsterdam: 1971.
35. Yi J, Thomas LM, Richter-Addo GB. Crystal Structure of Human *R*-State Aquomethemoglobin at 2.0 Å Resolution. Acta Cryst. F. 2011; 67:647–651.
36. Pflugrath J. The Finer Things in X-Ray Diffraction Data Collection. Acta Cryst. 1999; D55:1718–1725.
37. Leslie, AGW. Recent Changes to the MOSFLM Package for Processing Film and Image Plate Data; Joint CCP4 + ESF-EAMCB Newsletter on Protein Crystallography No. 26. 1992. p. 27-33.
38. Murshudov GN, Vagin AA, Dodson EJ. Refinement of Macromolecular Structures by the Maximum-Likelihood Method. Acta Cryst. 1997; D53:240–255.
39. Adams PD, Grosse-Kunstleve RW, Hung L-W, Loerger TR, McCoy AJ, Moriarty NW, Reed RJ, Sacchettini JC, Sauter NK, Terwilliger TC. PHENIX: Building New Software for Automated Crystallographic Structure Determination. Acta Cryst. 2002; D58:1948–1954.
40. Emsley P, Cowtan K. COOT: Model-Building Tools for Molecular Graphics. Acta Cryst. D. 2004; D60:2126–2132. [PubMed: 15572765]
41. Feng L, Gell DA, Zhou SP, Gu LC, Kong Y, Li JQ, Hu M, Yan N, Lee C, Rich AM, Armstrong RS, Lay PA, Gow AJ, Weiss MJ, Mackay JP, Shi Y. Molecular Mechanism of AHSP-Mediated Stabilization of α-Hemoglobin. Cell. 2004; 119:629–640. [PubMed: 15550245]
42. Vallone B, Nienhaus K, Matthes A, Brunori M, Nienhaus GU. The Structure of Carbonmonoxy Neuroglobin Reveals a Heme-Sliding Mechanism for Control of Ligand Affinity. Proc. Nat. Acad. Sci., USA. 2004; 101:17351–17356. [PubMed: 15548613]
43. Fago A, Crumbliss AL, Peterson J, Pearce LL, Bonaventura C. The Case of the Missing NO-Hemoglobin: Spectral Changes Suggestive of Heme Redox Reactions Reflect Changes in NO-Heme Geometry. Proc. Natl. Acad. Sci., USA. 2003; 100:12087–12092. [PubMed: 14514887]

44. Cheng, L.; Richter-Addo, GB. Binding and Activation of Nitric Oxide by Metalloporphyrins and Heme. In: Guilard, R.; Smith, K.; Kadish, KM., editors. The Porphyrin Handbook. Vol. Vol. 4. Academic Press; New York: 2000. p. 219-291.
45. Bunn HF, Jandl JH. Exchange of Heme Among Hemoglobin Molecules. Proc. Natl. Acad. Sci. USA. 1966; 56:974–978. (Addendum: p1926). [PubMed: 5230192]
46. Fujii M, Hori H, Miyazaki G, Morimoto H, Yonetani T. The Porphyrin-Iron Hybrid Hemoglobins - Absence of the Fe-His Bonds in One Type of Subunits Favors a Deoxy-Like Structure with Low-Oxygen Affinity. J. Biol. Chem. 1993; 268:15386–15393. [PubMed: 8340369]
47. Rachmilewitz EA. Formation of Hemichromes From Oxidized Hemoglobin Subunits. Ann. N. Y. Acad. Sci. 1969; 165:171–184. [PubMed: 4310790]
48. Bonnett R, Charalambides AA, Martin RA. Nitrosation and Nitrosylation of Haemoproteins and Related Compounds. Part 1. Porphyrins and Metalloporphyrins. J. Chem. Soc., Perkin Trans. 1978; 1:974–980.
49. Bonnett R, Hursthouse MB, Scourides PA, Trottter J. Nitrosation and Nitrosylation of Haemoproteins and Related Compounds. Part 3. Attack at the Vinyl Groups of Protoporphyrin Dimethyl Ester. X-Ray Analysis of 8^1(*E*)-8^2-Nitroprotoporphyrin Dimethyl Ester. J. Chem. Soc., Perkin Trans. 1980; 1:490–494.
50. Atassi MZ. Nitration of the Vinyl Groups of Ferriheme. Biochim. Biophys. Acta. 1969; 177:663–665. [PubMed: 5787258]
51. Lin HL, Myshkin E, Waskell L, Hollenberg PF. Peroxynitrite Inactivation of Human Cytochrome P450s 2B6 and 2E1: Heme Modification and Site-Specific Nitrotyrosine Formation. Chem. Res. Toxicol. 2007; 20:1612–1622. [PubMed: 17907788]
52. Williams DLH. *S*-Nitrosation and the Reactions of *S*-Nitroso Compounds. Chem. Soc. Rev. 1985; 14:171–196.
53. Gowenlock BG, Richter-Addo GB. Preparations of *C*-Nitroso Compounds. Chem. Rev. 2004; 104:3315–3340. [PubMed: 15250743]
54. Kunai A, Yanagi Y, Sasaki K. A Convenient Preparation of Conjugated Nitro Olefins by Electrochemical Methods. Tetrahedron Lett. 1983; 24:4443–4444.
55. Yandovskii VN, Ryabinkin II, Tselinskii IV. Formation of Nitro-Compounds during Nitrosation of Olefins by Alkylnitrites. Zh. Org. Khim. 1980; 16:2084–2086.
56. Jacob H, Winterhalter KH. Unstable Hemoglobins - Role of Heme Loss in Heinz Body Formation. Proc. Natl. Acad. Sci. USA. 1970; 65:697–701. [PubMed: 5267148]
57. Jacob HS, Winterhalter KH. Role of Hemoglobin Heme Loss in Heinz Body Formation - Studies with a Partially Heme-Deficient Hemoglobin and with Genetically Unstable Hemoglobins. J. Clin. Invest. 1970; 49:2008–2016. [PubMed: 5475984]
58. Winterhalter KH, Jacob HS. Heme Deficiency of Beta Chains: A Cause of Hemoglobin Precipitation in Congential Heinz Body Hemolytic Anemia (CHBHA). J. Clin. Invest. 1969; 48:A89. (Abstract No. 286).

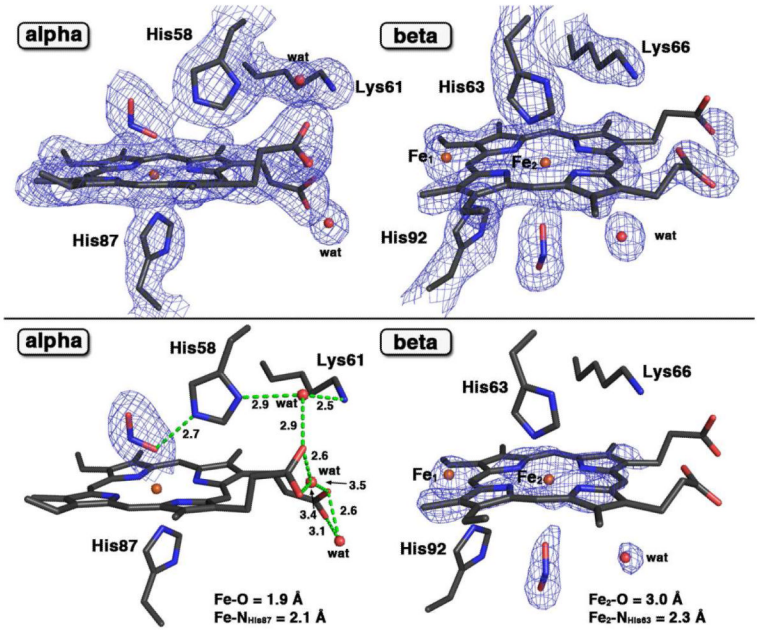

Figure 1.

(Top panel) The $2F_o$-F_c electron density maps (contoured at 1.0σ) and final models of the α- and β-heme active sites of the ferric human $Hb(ONO)_{d,p}$ structure (PDB accession code: 3ONZ, 2.1 Å resol.). (Bottom panel) The F_o-F_c omit electron density map (bottom, contoured at 3.0σ) and final models of the α- and β-heme active sites of this compound. The H-bonding interactions are shown in green dashed lines. The F_o-F_c omit electron density maps for water molecules in the α subunit are not shown here. Bonds to Fe are omitted for clarity.

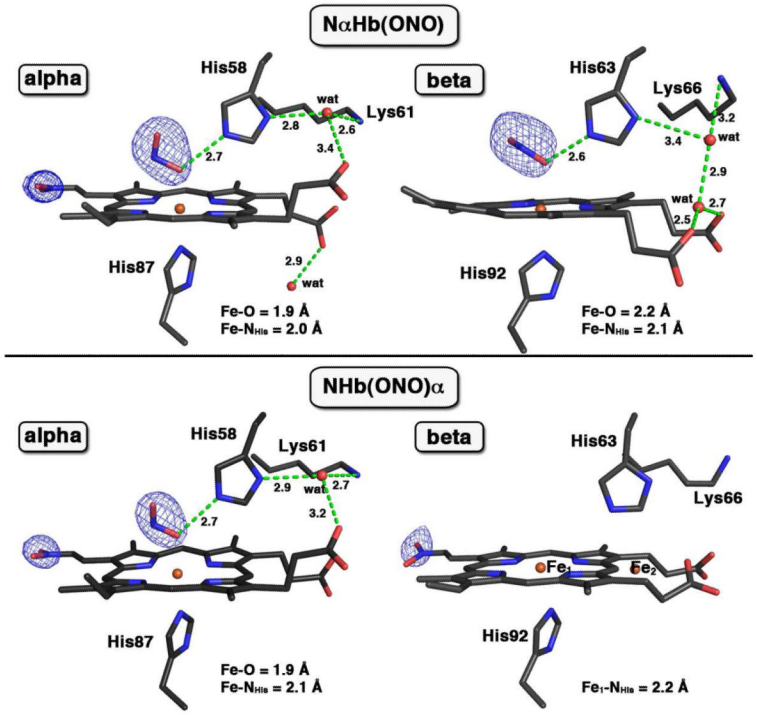

Figure 2.

F_o-F_c omit electron density maps (contoured at 3.0σ) and final model of the α- and β-heme active sites of two ferric human NHb nitrite adducts. The top panel is for NαHb(ONO) (PDB accession code: 3OO4, 1.9 Å resol.), and the bottom panel is for NHb(ONO)α (PDB accession code: 3OO5, 2.1 Å resol.). The two Fe atoms in the β subunit of NHb(ONO)α structure were modeled with an Fe–Fe distance of 4.6 Å. The H-bonding interactions are shown in green dashed lines, and bonds to Fe are omitted for clarity.

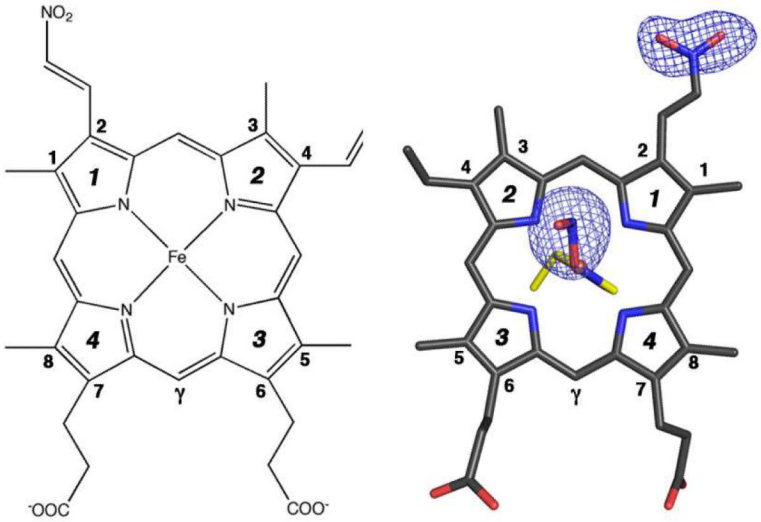

Figure 3.

(*Left*) The commonly used Fisher's numbering system for the protoporphyrin IX macrocycle. (*Right*) Top view of the F_o-F_c omit electron density map (contoured at 3.0σ) and final model of the a nitriheme and Fe-ONO moieties of NαHb(ONO). The proximal His87 residue is shown in yellow.

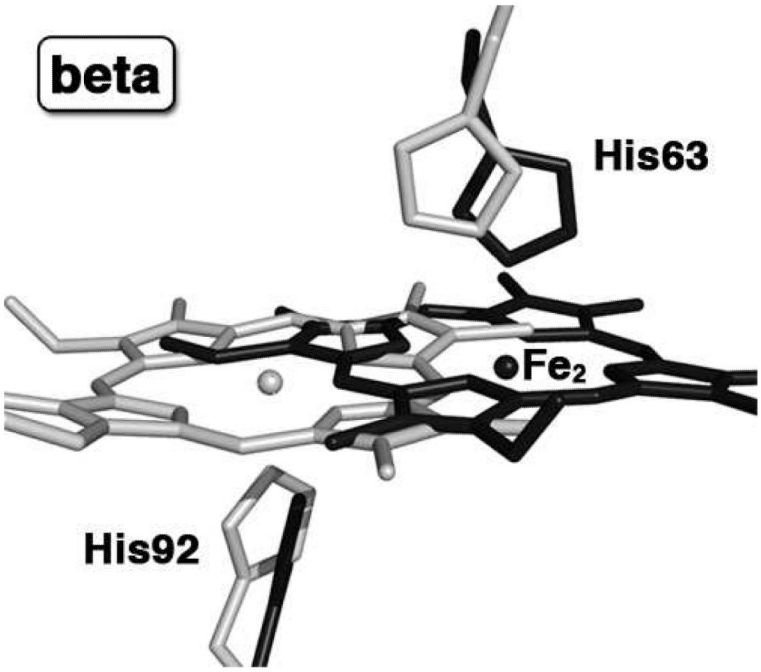

Figure 4.

The β heme sites of the superposed final models of our previously published HbONO structure (PDB accession code: 3D7O, 1.8 Å resol., shown in light gray) and new $Hb(ONO)_{d,p}$ structure (PDB accession code: 3ONZ, 2.1 Å resol., shown in black); for clarity, the Fe_1 and nitrite ligands are not shown.

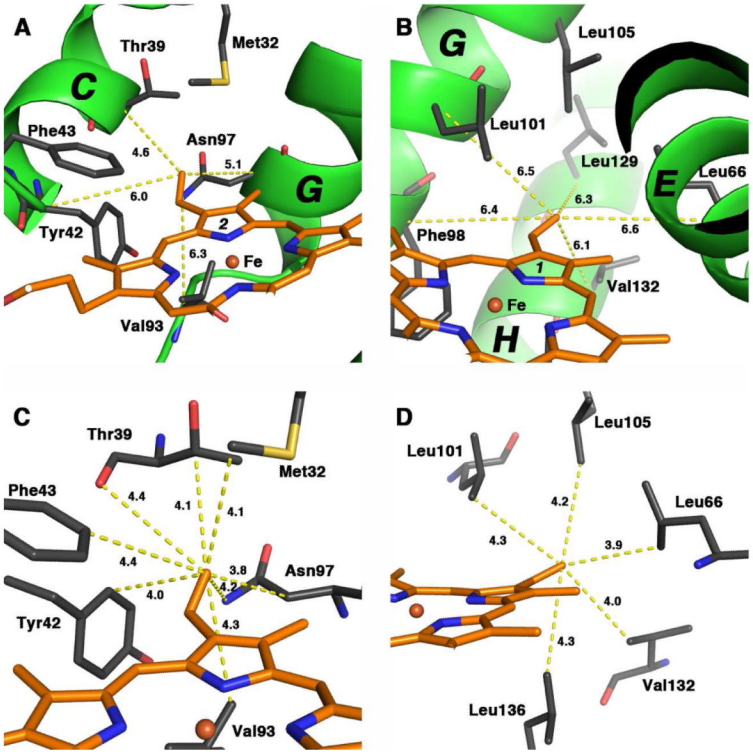

Figure 5.

The heme vinyl regions of the α subunit of ferric aquometHb (PDB accession code 3P5Q, 2.0 Å resol.). The close contacts between the terminal C*β* atoms at two vinyl positions of the α heme and the protein backbone C*α* atoms of the nearby residues (top panel) and the side chains of nearby residues (bottom panel) are shown as yellow dashed lines. (**A**) The close contacts of the terminal C*β* atom at the 4-vinyl position with the Cα atoms of nearby helices (e.g Helix C and Helix G); (**B**) The close contacts of the terminal C*β* atom at the 2-vinyl position with the C*α* atoms of nearby helices (Helix E, Helix G and Helix H); (**C**) The close contacts of the terminal C*β* atom at the 4-vinyl position with the side chains of nearby residues; (**D**) The close contacts of the terminal C*β* atom at the 2-vinyl position with the side chains of nearby residues.

Table 1

X-ray data collection and refinement statistics[a]

Name	$Hb(ONO)_{d,p}$	NαHb(ONO)	NHb(ONO)α
PDB Accession Code	3ONZ	3OO4	3OO5
A. Crystal parameters			
Space group	$P4_12_12$	$P4_12_12$	$P4_12_12$
Unit cell dimensions (Å)	53.3, 53.3, 193.6	53.5, 53.5, 190.0	53.5, 53.5, 192.2
Molecules per asymmetric unit	α1β1	α1β1	α1β1
Solvent content (%)	42.3	45.3	44.5
B. Data collection			
Wavelength (Å)	1.5418	1.5418	1.5418
Temperature (K)	100	100	100
Resolution range (Å)	46.7–2.09	27.3–1.9	27.5–2.1
Number of observations	156086	161544	217415
Unique reflections	16567	22776	17257
Average multiplicity	9.4 (9.4)	7.1 (5.23)	12.6 (12.6)
Completeness (%)	95.5 (90.7)	100 (100)	100 (100)
$\langle I/\sigma(I)\rangle$	29.3 (4.6)	12.7 (2.0)	14.6 (3.3)
R_{merge}[b]	0.053 (0.405)	0.057 (0.365)	0.053 (0.482)
C. Refinement			
Resolution (Å)	26.64–2.09	27.3–1.9	27.5–2.1
No. of reflections used	16540	22697	17179
No. of reflections used for R_{free}	856	1162	870
No. of protein atoms	2183	2287	2244
R-factor[c]	0.219	0.207	0.231
R_{free}[d]	0.287	0.263	0.287
Wilson B ($Å^2$)	39.1	32.8	48.2
rms deviations from ideal values[e]			
Bond lengths (Å)	0.02	0.01	0.01
Bond angles (°)	1.9	1.1	1.2
Ramachandran plot (%)[f]			
Favored region	93.7	98.2	97.5
Outliers	0.7	0	0
Rotamer outliers	4.1	0.9	1.8

[a] The data in brackets refer to the highest resolution shell.

[b] $R\text{merge} = \sum_{\square}\sum_i |I_{hi} - \langle I_h\rangle| / \sum_{\square}\sum_i |\langle I_h\rangle|$. I_{hi} is the ith used observation for unique hkl h, and $\langle I_h\rangle$ is the mean intensity for unique hkl h.

[c] $R = \sum||F_O| - |F_C|| / \sum|F_O|$ where F_O and F_C are the observed and calculated structure factors, respectively.

[d] R_{free} was calculated using 5% of the randomly selected diffraction data which were excluded from the refinement.

[e] Ideal values taken from: Engh, RA & Huber, R (1991) Accurate Bond and Angle Parameters for X-ray Protein Structure Refinement. *Acta Cryst.* A47: 392-400.

[f] calculated using *MolProbity* as implemented in *PHENIX*.